C_6^- Carbon Cluster Anion: An Infrared Absorption and Resonance Raman Isotopic Study

Jan Szczepanski, Edward Auerbach, and Martin Vala*

Department of Chemistry and Center for Chemical Physics, University of Florida, Gainesville, Florida 32611

Received: August 4, 1997; In Final Form: September 30, 1997[⊗]

The Fourier transform infrared and resonance Raman spectra of the C_6^- carbon cluster anion has been measured in argon matrices. Fundamental symmetric stretching modes have been observed at 2086, 1775, and 634 cm^{-1}, together with the overtone of a symmetric bending mode at 467 cm^{-1}. The major asymmetric stretching mode lies at 1936.7 cm^{-1}. Theoretical calculations utilizing Hartree−Fock (HF/6-31G*), Moller−Plesset perturbation (MP2/6-31G*), density functional (B3LYP/6-31G*), and quadratic configuration interaction QCISD/6-31G*, including triples QCISD(T)/6-31G*, support the assignment of these bands to the C_6^- cluster and indicate that it is linear with an acetylenic-like structure. Frequency shifts determined from infrared and resonance Raman studies of $^{12}C/^{13}C$ isotopically substituted C_6^- are generally in excellent agreement with the calculated isotopic frequency shifts, although not all isotopomeric bands were observed. The combination of resonance Raman and Fourier transform infrared spectroscopies with theoretical computations is shown to be a powerful approach for the study of carbon clusters and their anions.

I. Introduction

Carbon clusters are of current interest because of their integral part in soot, fullerenes, nanotubes, and astrophysics. While the bulk of the information currently available on small carbon clusters deals with neutral clusters, some work has been reported on carbon cluster ions. In particular, carbon clusters and their anions have been studied using a variety of experimental approaches: photoelectron spectroscopy,[1−3] zero kinetic energy spectroscopy,[4,5] gas-phase ion chromatography,[6] resonant multiphoton detachment spectroscopy,[7−9] photodissociation and photodetachment spectroscopy,[10] collision-induced dissociation,[11] electronic absorption[12] and emission,[13] and infrared spectroscopy[14,15] in rare gas matrices. Theoretical studies have been reported on several cluster anions.[16−20] Some studies have dealt with the vibrational frequencies of carbon cluster anions,[1,2,7,13,19] but usually only symmetric mode frequencies in excited electronic states have been specified. Some work has been reported on ground-state symmetric modes, usually gotten indirectly from hot band structure. The asymmetric modes of some small linear carbon cluster anions C_n^- ($n < 10$, $n \neq 8$) in Ar matrices[14,20] and C_n^- ($n = 5-10$, 12) in Ne matrices[15] were recently investigated via infrared spectroscopy.

Fourier transform IR absorption spectroscopy of small neutral isotopically labeled carbon clusters isolated in noble gas matrices has been very successfully used in the past for the identification of the size and structure of specific clusters.[22−28] This technique can be used for the study of ionic carbon cluster species as well. Very recently we reported on $^{12/13}C$ isotopic studies of the ν_3 mode of the C_3^- carbon cluster. An analysis of its six isotopomeric bands established its linear structure.[21]

In our recent study of carbon cluster anions,[14] an IR band at 1936.7 cm^{-1} (in Ar) was assigned to the $\nu_4(\sigma_u)$ asymmetric stretching mode of the linear C_6^- cluster anion. This assignment was based on the following: (1) an energy threshold of 4.7 eV for photobleaching of the 1936.7 cm^{-1} absorption band was found. This energy was linked to the 4.185 eV electron detachment energy[2] of gaseous C_6^-, with the higher energy in Ar matrices due to the stabilization of the C_6^- ions in the matrix. (2) A good intensity correlation was found between the $C^2\Pi_g - X^2\Pi_u$ (0^0_0) electronic transition of C_6^- at 615.8 nm (in Ar) and the IR band at 1936.7 cm^{-1}. (3) The calculated $\nu_4(\sigma_u)$ transition using B3LYP/6-31G* density functional theory (scaled by 0.95) matches the 1936.7 cm^{-1} experimental frequency and shows a large calculated intensity (726 km/mol). Also very recently Freivogel et al.[15] reported the 1938.5 cm^{-1} ν_4 mode frequency for C_6^- in a Ne matrix.

To support this IR assignment and to study the C_6^- cluster further, we present here an infrared and resonance Raman study of isotopically labeled C_6^- cluster anions. Isotopic mixtures have long been used in infrared investigations on molecules of unknown structure. We apply this approach also to resonance Raman spectra of the C_6^- cluster. It is shown that the use of isotopic mixtures gives rise, upon excitation with a single laser wavelength, to a Raman spectrum composed of spectrally dispersed bands of all isotopomers simultaneously. Comparison of the observed Raman and infrared bands to density functional calculational results lends strong support to our band assignments. The combined use of resonance Raman spectroscopy, infrared spectroscopy, and density functional theory calculations is shown to provide a powerful approach to the study of any small clusters.

II. Computational Methods

Geometry optimization (yielding optimum bond lengths) and harmonic vibrational frequencies for linear ground-state $^{12}C_6^-$ were calculated using the GAUSSIAN 94 program package.[29] In our earlier study,[14] stable structures for both the linear and cyclic isomers of C_6^- were calculated using B3LYP/6-31G* theory. The linear structure was found to be more stable than the cyclic (D_{3h}) by 149.8 kJ/mol. The predicted infrared frequency (B3LYP/6-31G*, scaled by 0.95) for cyclic C_6^- falls in the 1530 cm^{-1} region, far from the observed 1936.7 cm^{-1} anion band position. Thus, it was concluded that linear C_6^- was responsible for the 1936.7 cm^{-1} IR band. To investigate this conclusion further, calculations employing Hartree−Fock (HF/6-31G*), Moller−Plesset perturbation (MP2/6-31G*), density functional (B3LYP/6-31G*), and quadratic configuration interaction QCISD/6-31G*, including triples QCISD(T)/6-31G*, were performed to determine the optimum geometry and cluster vibrational frequencies. The results of these calculations are given in Table 1. The computed bond lengths show that a single−triple bond alternation is preferred by all methods. The

[⊗] Abstract published in *Advance ACS Abstracts,* November 15, 1997.

S1089-5639(97)02547-4 CCC: $14.00

TABLE 1: Calculated Stretching Frequencies (Unscaled, in cm^{-1}) of Linear C_6^-, Intensities (in Brackets, in km/mol), Bond Lengths (*R* in Å), and Rotational Constants (*B* in GHz). A 6-31G* Basis Set Was Used in All Calculations

parameter	UHF	MP2	B3LYP[a]	QCISD
$\nu_1(\sigma_g)$	2411.9[0]	2175.1[0]	2193.2[0]	2235.6[0]
$\nu_2(\sigma_g)$	2024.7[0]	1947.0[0]	1865.4[0]	1869.1[0]
$\nu_3(\sigma_g)$	697.4[0]	661.3[0]	657.9[0]	654.5[0]
$\nu_4(\sigma_u)$	2158.9[3663]	1971.5[828]	2036.6[726]	2024.9[1662]
$\nu_5(\sigma_u)$	1296.5[0.6]	1238.1[20]	1222.4[1]	1216.1[1]
R_1(Å)[b]	1.2565	1.2773	1.2782(1.275[c])	1.2820(1.290[d])
R_2(Å)[b]	1.3299	1.3320	1.3293(1.325[c])	1.3372(1.337[d])
R_3(Å)[b]	1.2331	1.2645	1.2569(1.252[c])	1.2576(1.266[d])
B(GHz)		1.42610	1.432485	1.421836

[a] Reference 14. [b] Bonds lengths are numbered from the outer to the central C−C bond. [c] RCCSD(T)/204c GTO level of theory, ref 19. [d] QCISD(T)/6-31 G*, this work.

B3LYP and QCISD results of the computed stretching frequencies agree rather closely, while the HF and MP2 results agree less well.

Isotopic frequency shift calculations were also undertaken with B3LYP and QCISD methods. In these calculations, the geometry and force constants were adopted unchanged from the $^{12}C_6^-$ cluster results. The computed values of the spin angular momentum quantum number, $\langle S^2 \rangle$, are 0.769 (HF), 0.762 (MP2), 0.750 (B3LYP), and 0.770 (QCISD), indicating almost no spin contamination in these calculations.

III. Experimental Methods

The dual laser beam experimental setup used for generation of $^{12/13}C_6^-$ carbon cluster ions is the same as that used in the C_3^- cluster studies reported earlier.[21] In brief, the 1064 nm fundamental from a Nd:YAG laser is dispersed from the 532 nm second harmonic beam and, in part, focused on a piece of yttrium metal, thereby generating a violet/blue Y/Ar plasma. Carbon clusters (including C_6) formed by ablation of a pressed powder of a $^{12}C/^{13}C$ pellet by the 532 nm second harmonic beam readily trap electrons from the plasma. The negatively charged clusters are partially extracted from the vaporization region and co-condensed with Ar matrix gas on a BaF_2 cryostat window (IR absorption) or on a Al-coated copper block attached to a cryostat coldfinger (resonance Raman). To increase the concentration of C_6 vs C_3 clusters, a higher photon flux of the carbon-ablating 532 nm beam was used than in the C_3^- experiments.[21] For the above experimental conditions, no yttrium-bearing species was observed in the 4000−750 cm^{-1} region. The 1064 nm photon flux on the yttrium surface was just above threshold for plasma initiation. Even after a 1 h deposit (10 Hz laser repetition rate), no substantial yttrium loss from the surface could be observed. The electron photodetachment process of $^{12/13}C_6^-$ during photolysis (Hg lamp, 100 W, full spectral output) caused a bleaching of the anion bands. This was helpful in identifying the isotopomer absorption bands of $^{12/13}C_6^-$ in the region where neutral and anion $^{12/13}C_6$ cluster spectra overlap.

The absorption spectra of carbon species isolated in solid Ar were probed in the IR region using a MIDAC Fourier transform infrared spectrometer with 0.7 cm^{-1} resolution.

The resonance Raman spectra of $^{12/13}C_6^-$ carbon cluster ions were measured using a CW dye laser (Spectra Physics 375B) as the Raman excitation source. The dye laser beam was spectrally filtered using a highly dispersive prism located 2 m from a pinhole. This removed the fluorescence and amplified spontaneous emission from the lasing dye. Spectra were collected on a Spex 1700 3/4m double monochromator (1 cm^{-1} resolution), with a cooled RCA C31034 photomultiplier tube using standard photon-counting electronics.

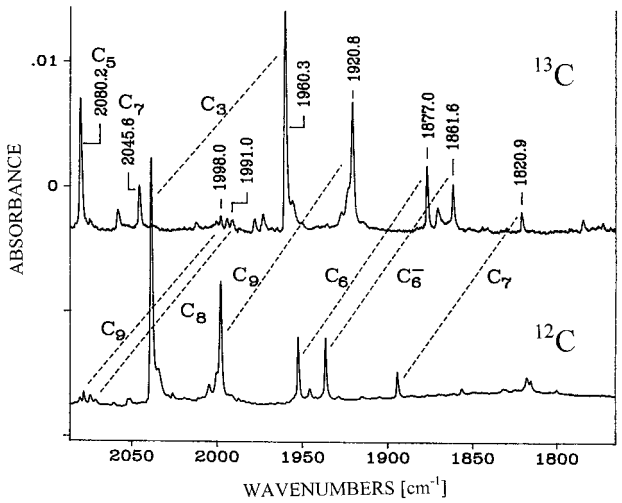

Figure 1. Portion of the IR spectrum of C_n and C_6^- carbon clusters recorded for a laser-ablated ^{13}C isotope sample (upper spectrum) and ^{12}C isotope sample (lower spectrum). The frequencies of marked bands in the lower spectrum are 2078.0 cm^{-1} ($^{12}C_9$, $\nu_5(\sigma_u)$),[30] 2071.5 cm^{-1} ($^{12}C_8$, $\nu_5(\sigma_u)$),[30] 2038.9 cm^{-1} ($^{12}C_3$, $\nu_3(\sigma_u)$),[22] 1998.0 cm^{-1} ($^{12}C_9$, $\nu_6(\sigma_u)$),[26] 1952.5 cm^{-1} ($^{12}C_6$, $\nu_4(\sigma_u)$),[24] 1936.7 cm^{-1} ($^{12}C_6^-$, $\nu_4(\sigma_u)$),[14] and 1894.3 cm^{-1} ($^{12}C_7$, $\nu_5(\sigma_u)$).[26]

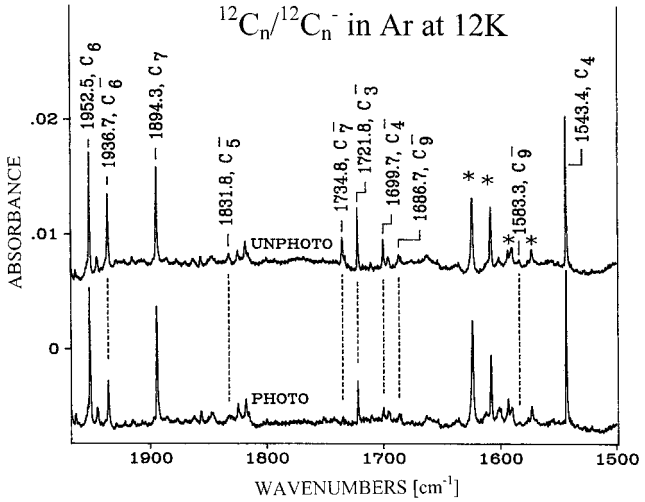

Figure 2. Effect of photolysis (20 min,100 W Hg lamp, full spectral output) on the IR band intensities of the C_n^- ($n < 10$) carbon cluster anions and neutrals. Bands marked with a * are due to isolated water.

IV. Results and Discussion

a. Infrared Absorption. Figure 1 presents IR absorption spectra in the 2000 cm^{-1} region for clusters ($^{12}C_n/^{12}C_n^-$ and $^{13}C_n/^{13}C_n^-$) formed from the pure isotopes and isolated in Ar matrices at 12 K. The bottom spectrum shows, among numerous others, the 1936.7 cm^{-1} band previously assigned to linear $^{12}C_6^-$. The band assignments in the ^{13}C spectrum (top) are based on the ^{12}C spectrum by accounting for the isotopic frequency shifts expected from the Redlich−Teller formula. The band intensity changes during photolysis were also taken into account (vide infra).

Upon photolysis (20 min, 100 W Hg lamp, full spectral output), all bands assigned to the cluster anions declined in intensity, including the 1936.7 cm^{-1} C_6^- cluster band, while the neutral cluster bands were not much affected (cf. Figure 2). A newly observed band at 2064 cm^{-1} also declined in intensity and is here tentatively assigned to the ν_5 (σ_u) asymmetric

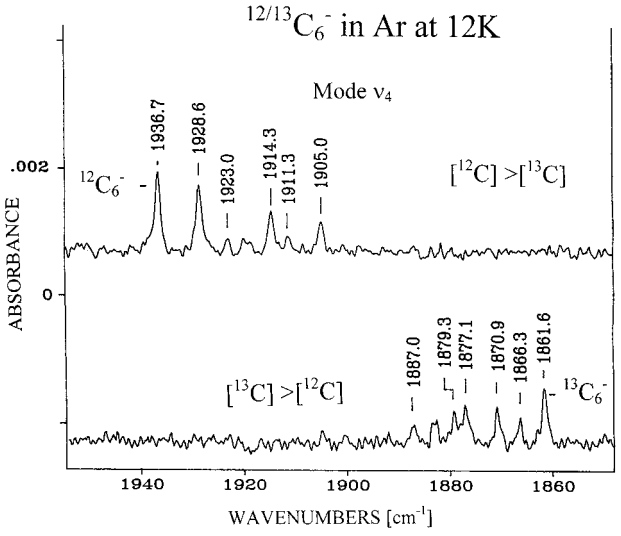

Figure 3. IR absorption spectra (in Ar) of ^{12}C and ^{13}C isotopically labeled C_6^- carbon cluster ions recorded for [^{12}C] > [^{13}C] (upper spectrum) and for [^{12}C] < [^{13}C] concentration cases (lower spectrum). The spectra were obtained by subtraction of an after-photolysis (1 h, unfiltered 100 W Hg lamp) spectrum from a before- photolysis spectrum of a C_n/C_n^-/Ar matrix.

stretching mode of linear C_8^-. The calculated harmonic frequency for the most intense IR mode of linear C_8^- (B3LYP/6-31G*, scaled by 0.958) matches exactly the observed band frequency.[14]

In addition to the pure isotopic runs in Figure 1, several other isotopic mixtures were used to determine the isotopic frequency pattern for C_6^-. Two concentration mixtures (one with [^{12}C]>[^{13}C] (ca. 4:1) and the other with [^{12}C]<[^{13}C] (ca. 1:4)) were used. These mixtures plus the decrease in band intensity of the anions with photolysis were helpful in distinguishing the $^{12/13}C_6^-$ ν_4 asymmetric mode isotopomer bands from the neutral $^{12/13}C_6$ cluster isotopomer bands in the overlapped 1936.7−1861.6 cm^{-1} region. For each mixture an "after-photolysis" spectrum was subtracted from a "before-photolysis" run; the subtraction spectra are shown in Figure 3. Interestingly, not all 36 expected isotopomeric bands attributable to C_6^- appear. This results from the isotopic ratios used to form the cluster and from the overlapping of some isotopomer bands. The positions of the observed groups of bands are, however, consistent with the frequencies of the predicted bands. Table 2 gives the proposed assignments of the observed bands. (The complete listing of all 36 calculated isotopomeric frequencies of linear $^{12/13}$ C_6^- is available from the authors upon request.)

The strongest bands in Figure 3 are due to isotopomers with either all-^{12}C or singly-^{13}C-substituted C_6^- clusters (upper spectrum) or all-^{13}C and singly-^{12}C-substituted isotopomers (lower). The agreement between calculated and observed band frequencies is reasonably good (cf. Table 2). The 1928.6 cm^{-1} band in Figure 2 is almost as intense as the 1936.7 cm^{-1}(12−12−12−12−12−12) band. It probably results from three isotopomers, 12−12−**13**−12−12−12, **13**−12−12−12−12−12, and 12−12−**13**−**13**−12−12, for which the calculated (B3LYP/6-31G*) scaled frequencies are 1931.7, 1928.8, and 1928.4 cm^{-1}, respectively. The other small intensity bands observed in the figure are tentatively assigned to the following doubly and triply substituted isotopomers of C_6^-: 1923.0 cm^{-1} (**13**−12−12−**13**−12−12 and **13**−12−**13**−12−12−12), 1911.3 cm^{-1} (12−**13**−12−**13**−12−12 and **13**−12−**13**−**13**−12−12), and 1905.0 cm^{-1} (12−**13**−**13**−12−12−12, **13**−12−12−12−**13**−12, and 12−**13**−**13**−**13**−12−12). Other proposed assignments are given in Table 2.

TABLE 2: Experimental (Ar/12 K) and Theoretical (B3LYP/6-31G* and QCISD/6-31G*) Isotopomer Asymmetric ν_4 Stretching Mode Frequencies (in cm^{-1}) for the Linear C_6^- Anion

expt.	isotopomer	B3LYP[a]	QCISD[b]
1936.7	12−12−12−12−12−12	1936.7	1936.7
1928.6	12−12−**13**−12−12−12	1931.7	1932.0
	13−12−12−12−12−12	1928.8	1928.9
	12−12−**13**−**13**−12−12	1928.4	1928.5
1923.0	**13**−12−12−**13**−12−12	1924.9	1925.2
	13−12−**13**−12−12−12	1922.4	1922.8
1920.0	**13**−12−12−12−12−**13**	1920.1	1920.0
1914.3	12−**13**−12−12−12−12	1913.3	1913.7
1911.3	12−**13**−12−**13**−12−12	1911.4	1911.8
	13−**12**−13−13−**12**−12	1911.2	1911.1
1905.0	12−**13**−**13**−12−12−12	1904.0	1905.3
	13−12−12−12−**13**−12	1903.4	1903.5
1887.0	12−**13**−12−12−**13**−12	1886.9	1886.8
	13−**12**−13−13−13−13	1886.3	1886.9
1879.3	12−**13**−12−12−**13**−**13**	1878.9	1878.8
1877.1	**12**−13−13−13−13−**12**	1878.6	1878.5
1870.9	**12**−13−13−13−13−13	1870.2	1870.1
	13−13−**12**−**12**−13−13	1869.7	1869.4
1866.3	13−13−**12**−13−13−13	1864.4	1864.4
1861.6	13−13−13−13−13−13	1860.7	1860.5

[a]The scaling factor for the B3LYP method was 0.950. [b]The scaling factor for the QCISD method was 0.956.

The assignment of specific isotopomers to the experimental bands in $^{12/13}C_6^-$ is not as straightforward as for the $^{12/13}C_3^-$ spectra, reported previously.[21] For the $^{12/13}C_6^-$ clusters, the calculated vibrational frequencies are very sensitive to ^{13}C substitution at the different levels of theory employed, especially when the calculated σ_u modes are close in energy to the σ_g modes. This can lead to intensity "sharing" in "broken symmetry" isotopomers. For example, in the MP2 calculations, the frequency of the $\nu_2(\sigma_g)$ mode is very close to the $\nu_4(\sigma_u)$ mode (only 24.5 cm^{-1} distant, cf. Table 1). In the 12−**13**−12−12−12−12 anion, the vibrational motions for the above modes can no longer be classified as g or u symmetry. By breaking the symmetry in this isotopomer the first mode "borrows" 60% intensity from the second one. This mode mixing influences the calculated frequency also. Using MP2/6-31G* level theory (scaled to the ν_4 experimental frequency), it is 10 cm^{-1} higher than that calculated at the B3LYP/6-31G* level and 9.5 cm^{-1} higher than from the QCISD/6-31G* output. This illustrates that calculated isotopic frequency shifts should be handled with care when comparing them to experimental shifts, particularly in those cases where calculated mode energies are very close in value. A similar observation has already been made in studies of the neutral $^{12/13}C_7$ and $^{12/13}C_9$ carbon clusters.[27,28]

b. Resonance Raman. The inset in Figure 4 shows the electronic absorption in the origin region of the $^{12}C_6^-$ $C^2\Pi_g-X^2\Pi_u$ transition. This closely matches previous work.[12] Excitation into the 0_0^0 band (at 615.8 nm in Ar) results in the resonance Raman signal observed in Figure 4. Symmetric stretching modes can be noted at 634 cm^{-1}, $\nu_3(\sigma_g)$; 1775 cm^{-1},$\nu_2(\sigma_g)$; and 2086 cm^{-1} $\nu_1(\sigma_g)$. These bands are observed in the ratio 1:0.01:0.24, respectively . The band at 1261 cm^{-1} is assigned to 3_2^0, two quanta of vibration in the $\nu_3(\sigma_g)$ mode, while the band at 467 cm^{-1} is assigned to 8_2^0, two quanta of the π_g bending vibration. These assignments are given in Table 3. Calculated harmonic frequencies (B3LYP/6-31G* level, all scaled to the $\nu_4(\sigma_u)$ experimental mode frequency by the factor 0.9509) are 625.6 (ν_3), 1773.9 (ν_2), and 2085.6 cm^{-1} (ν_1). These observed frequencies may also be compared to the anharmonic frequencies of 634 (ν_3), 1790 (ν_2), and 2124 cm^{-1} (ν_1) calculated by Schmatz and Botschwina.[19] These workers stated that the ν_1

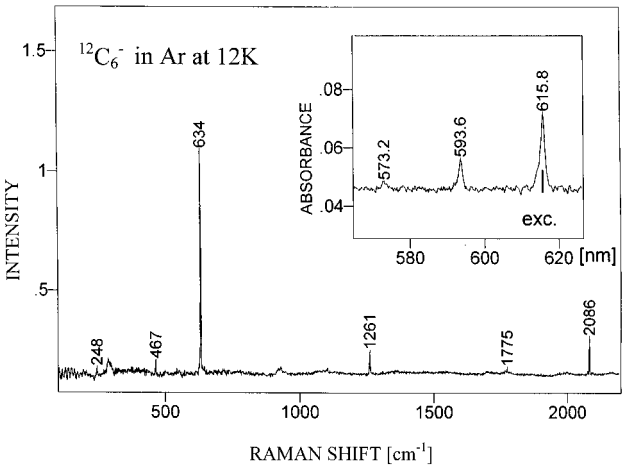

Figure 4. Resonance Raman spectrum of $^{12}C_6^-$ in Ar matrix at 12K. The 16237 cm^{-1} excitation line position is marked on the $C^2\Pi_g - X^2\Pi_u$-(0^0_0) electronic absorption spectrum of $^{12}C_6^-$ (inset spectrum). The 2086, $\nu_1(\sigma_g)$, 1775, $\nu_2(\sigma_g)$, and 634 cm^{-1}, $\nu_3(\sigma_g)$ fundamental modes of the $^{12}C_6^-$ cluster in the $X^2\Pi_u$ state are marked. The 1261 cm^{-1} band is due to the $2\nu_3(\sigma_g)$ vibration.

TABLE 3: Resonance Raman Bands of C_6^- (Ar/12 K) and Calculated Symmetric Vibrational Frequencies (in cm^{-1}) at the B3LYP/6-31G* and RCCSD(T)/204c GTOs Levels of Theory

		theory		
ν_{exp}	assignment	B3LYP (unscaled)	B3LYP[a] (scaled)	RCCSD(T)[b] (unscaled)
248				
467	8_2^0			
634	3_1^0	657.9	625.6	634
1261	3_2^0			
1775	2_1^0	1865.4	1773.9	1790
2086	1_1^0	2193.2	2085.6	2124

[a] Scaled by a factor of 0.9509. [b] Reference 19.

mode frequency was overestimated. Nevertheless, there is excellent agreement between the calculated and experimental values and between the two sets of calculated results.

Confirmation of these assignments can be gotten from resonance Raman spectra of a $^{12}C/^{13}C$ isotopically labeled sample. The electronic origins of all 36 possible isotopomers of C_6^- are apparently shifted by less than the bandwidth (fwhm) of the 0_0^0 band, which is 20 cm^{-1}, as shown in Figure 4. Excitation with a single laser line may thus be able to excite all 36 isotopomers simultaneously, depending, of course, on the concentration and effective absorption of each particular isotopomer at the excitation wavelength used. Two different isotopic concentration mixtures were used here. In one mixture $[^{12}C] > [^{13}C]$ (ca. 4:1), and in the other, the mixture was reversed, i.e., $[^{12}C] < [^{13}C]$ (ca. 1:4). The resonance Raman spectra obtained from these ablated mixtures are shown in Figure 5. From a comparison of the observed spectrum to the calculated $^{12/13}C_6^-$ isotopomer frequency shifts, it is clear that both the pure $^{12}C_6^-$ and $^{13}C_6^-$ isotopomers were selected in the resonance Raman process. As will be seen, it is probably safe to assume that the remaining 34 isotopomers, whose absorption band maxima lie between these two, were also selected.

For the more intense 634.0 cm^{-1} parent, five "bands" or groups of bands are clearly discernible. This is, however, far from the expected 36 bands! Two factors limit the number of observed bands. First, the isotopic concentrations chosen tend to limit the abundance of certain isotopomers, i.e., to those containing only one or two of the least abundant isotope. And, second, as Table 4 shows, a number of isotopomers are expected

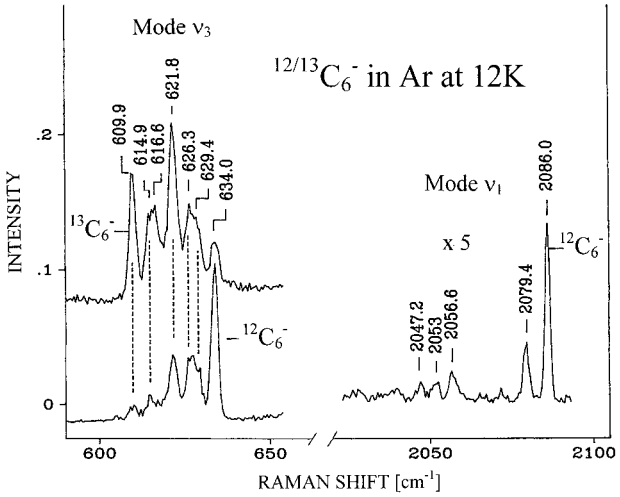

Figure 5. Resonance Raman spectra of isotopically mixed $^{12/13}C_6^-$ carbon cluster anions in Ar (12 K) for the ν_1 and ν_3 stretching modes. Lower spectrum shows both ν_1 and ν_3 modes of C_6^- obtained from an isotopic graphitic mixture with $[^{12}C] > [^{13}C]$ and upper spectrum shows only the ν_1 mode obtained with $[^{13}C] > [^{12}C]$. Excitation energy of 16233 cm^{-1} from a 50 mW CW dye laser with a 1 cm^{-1} fwhm laser line width was employed.

TABLE 4: Experimental (Ar/12 K) and Theoretical (B3LYP/6-31 G* and QCISD/6-31G*) Isotopomeric ν_3 Stretching Mode Frequencies (in cm^{-1}) for C_6^- Anion

expt.	isotopomer	B3LYP[a]	QCISD[b]
634.0	12−12−12−12−12−12	634.0	634.0
	12−12−13−12−12−12	633.7	633.7
	12−12−13−13−12−12	633.3	633.4
629.4	12−13−12−12−12−12	629.4	629.4
	12−13−13−12−12−12	629.1	629.1
	12−13−12−13−12−12	629.0	629.0
	12−13−13−13−12−12	628.7	628.8
626.3	13−12−12−12−12−12	626.0	626.0
	13−12−13−12−12−12	625.7	625.7
	13−12−12−13−12−12	625.6	625.6
	13−12−13−13−12−12	625.3	625.3
	12−13−12−12−13−12	624.8	624.7
	12−13−12−13−13−12	624.4	624.4
	12−13−13−13−13−12	624.1	624.1
621.8	13−13−12−12−12−12	621.7	621.7
	13−13−13−12−12−12	621.5	621.5
	13−12−12−12−13−12	621.4	621.4
	13−13−12−13−12−12	621.3	621.3
	12−13−12−13−12−13	621.1	621.1
	12−12−13−13−13−13	621.1	621.1
	12−13−13−12−12−13	621.1	621.1
	12−13−13−13−12−13	620.8	620.8
616.6	13−12−12−12−12−13	618.1	618.1
	13−12−12−13−12−13	617.9	617.8
	13−12−13−13−12−12	617.6	617.5
	12−13−12−12−13−13	617.1	617.1
	13−13−13−12−13−13	616.8	616.9
	12−13−12−13−13−13	616.9	616.7
	12−13−13−13−13−13	616.5	616.5
	13−12−12−12−13−13	616.5	613.9
	13−13−13−12−12−13	613.7	613.6
	13−13−12−13−12−13	613.6	613.5
614.9	13−12−13−13−13−13	613.3	613.3
	13−13−12−12−13−13	609.7	609.6
	13−13−12−13−13−13	609.4	609.3
609.9	13−13−13−13−13−13	609.1	609.0

[a] Scaling factor was 0.950. [b] Scaling factor was 0.956.

to exhibit overlapping frequencies. The calculated ν_3 frequencies for all 36 isotopomers can be seen to fall into several distinct groups. These groups vary in frequency spread from 0.7 to 1.9 cm^{-1}. The greater intensity of the 621.8 cm^{-1} band probably results from the contributions of eight different isotopomers,

TABLE 5: Experimental (Ar/12 K) and Theoretical (B3LYP/6-31G* and QCISD/6-31G*) Isotopomeric Symmetric ν_1 Stretching Mode Frequencies (in cm^{-1}) for the C_6^- Anion

expt.	isotopomer	B3LYP	QCISD
2086.0	12−12−12−12−12−12	2086.0	2086.0
	13−12−12−12−12−12	2085.0	2085.0
2079.4	12−**13**−12−12−12−12	2079.3	2078.9
	13−**13**−12−12−12−12	2078.8	2078.3
	13−12−12−12−**13**−12	2078.0	2077.7
2056.6	12−12−**13**−12−12−12	2056.9	2056.5
	13−12−**13**−12−12−12	2056.0	2055.4
	13−12−12−**13**−12−12	2055.1	2054.8
2053.0	12−**13**−**13**−12−12−12	2051.6	2050.3
	13−**13**−**13**−12−12−12	2051.3	2049.7
2047.2	12−**13**−12−**13**−12−12	2047.0	2046.9
	13−**13**−12−**13**−12−12	2046.1	2045.9
	12−**13**−12−**13**−12−**13**	2045.7	2045.5

TABLE 6: Observed Fundamental Mode Frequencies (in cm^{-1}) of the $X^2\Pi_u$ Electronic State and the $C^2\Pi_g$ Electronic Excited State of the Linear $^{12}C_6^-$ Anion

	$X^2\Pi_g$ State		$C^2\Pi_u$	
mode assignment	gas phase[a]	Ar matrix[b]	gas phase[a]	Ne matrix[c]
$\nu_1(\sigma_g)$		2086	2052	2064
$\nu_2(\sigma_g)$		1775	1767	
$\nu_3(\sigma_g)$	564[d]	634	602	607/605 Ar[f]
$\nu_4(\sigma_u)$		1936.7/1938.5[h]		
ν_7	220[g]			
$\nu_8(\pi_g)$	201[d]	∼233[e]	245	
$\nu_9(\pi_u)$	111[g]		110	

[a] From electron detachment spectra, ref 7. [b] This work. ±0.2 cm^{-1} for σ_u mode and ±2 cm^{-1} for σ_g modes. [c] From electronic absorption spectra, ref 12. [d] From hot bands, ref 7. [e] Tentative assignment based on the 467 cm^{-1} observed band. [f] From the insert spectrum of Figure 5 (this work). [g] Reference 5. [h] Ne matrix, ref 15.

of which the two containing three ^{12}C and three ^{13}C atoms can be expected to be smaller contributors. The difference in band shape, particularly for the 634.0 cm^{-1} band, between the two different concentration runs is interesting. With a greater concentration of ^{12}C-bearing isotopomers, the lower spectrum exhibits a more intense peak than the upper one with a higher concentration of ^{13}C-containing isotopomers. This can be accounted for if the lower run arises predominantly from the all-^{12}C species, while in the upper run each of the three isotopomers contribute more or less equally. The reverse would be true for the 609.9 cm^{-1} band.

For the weaker 2086 cm^{-1} band, Figure 5 (right side) also shows only five bands. Only the spectrum whose isotopic mixture [^{12}C] ≫ [^{13}C] is shown; the run with the reverse ratio was too weak to be seen. Table 5 lists the observed bands as well as the predicted frequencies for isotopomers between 2086.0 and 2045.0 cm^{-1}. It can be seen that the predicted isotopomeric peaks fall into five distinct classes. If one assumes that the isotopomer containing the fewest ^{13}C carbons (highlighted in the table) contributes the most intensity to the band, the match is excellent.

V. Summary of Vibrational Assignments

Table 6 summarizes the known fundamental mode frequencies for C_6^- in its electronic ground and $C^2\Pi_u$ excited states. The excited C state vibrations were reported from electronic absorption spectra in Ne matrices[12] and from one-color electron photodetachment spectra in the gas phase.[7]

In general, electronic excitation lowers molecular vibrational frequencies. This also occurs for C_6^- anions where Table 6 shows an 8−34 cm^{-1} frequency lowering in the electronic excited state. The gas-phase band at 564 cm^{-1} assigned[7] from a hot band analysis to the $\nu_3(\sigma_g)$ mode in the electronic ground state is problematic. The same mode in an Ar matrix falls at 634 cm^{-1}. The 70 cm^{-1} shift between matrix and gas phase appears to be too high and in the wrong energy direction. This assignment is also not consistent with the observation that the same mode in the C excited state is almost isoenergetic in both the Ne matrix and the gas phase (cf. Table 6). A 1817 cm^{-1} band, observed in Ne matrices and assigned by Freivogel et al.[12] to the $\nu_2(\sigma_g)$ mode of the C state, was later reassigned by Schmatz and Botschwina to the 3_0^3 vibration.[19]

From the spectra in Figure 4, the band at 1261 cm^{-1} is mostly likely due to 3_2^0, a two quanta vibration in the $X^2\Pi_g$ electronic ground state. For linear C_6^- clusters the symmetrical bending motion is expected be seen in the resonance Raman spectrum as a two-quanta vibration. The 467 cm^{-1} band (cf Figure 4) is close in energy to the expected 8_2^0 π_g vibration. This assignment is based on the calculated frequency of ca. 270 cm^{-1} (B3LYP/6-31G*, scaled by 0.95) and ca. 245 cm^{-1} (QCISD/6-31G*, scaled by 0.956). Thus we propose that the 233 cm^{-1} band is due to the 8_1^0 fundamental symmetrical bending vibration of the C_6^- cluster.

In summary, FTIR and resonance Raman(RR) spectra have been obtained for C_6^- in Ar matrices yielding major bands (and their symmetries) at 2086 cm^{-1} ($\nu_1(\sigma_g)$), 1775 cm^{-1} ($\nu_2(\sigma_g)$), 634 cm^{-1} ($\nu_3(\sigma_g)$), and 1936.7 cm^{-1} ($\nu_4(\sigma_u)$). An RR band at 467 cm^{-1} has also been assigned to a two-quanta vibration of the ν_8 bending mode.

Acknowledgment is made to the National Aeronautics and Space Administration and the donors of the Petroleum Research Fund, administered by the American Chemical Society, for their support of this research.

References and Notes

(1) Yang, S.; Taylor, K. J.; Craycraft, M. J.; Conceicao, J.; Pettiette, C. L.; Cheshnovsky, O.; Smalley, R. E. *Chem. Phys. Lett.* **1988**, *144*, 431.
(2) Arnold, D. W.; Bradforth, S. E.; Kitsopoulos, T. N.; Neumark, D. M. *J. Chem. Phys.* **1991**, *95*, 8753.
(3) Handshuh, H.; Gantefor, G.; Kessler, B.; Bechthold, P. S.; Eberhardt, W. *Phys. Rev. Lett.***1995**, *77*, 1095.
(4) Kitopoulos, T. N.; Chick, C. J.; Zhao, Y; Neumark, D. M. *J. Chem. Phys.* **1991**, *95*, 5479.
(5) Arnold, C. C.; Zhao, Y.; Kitopoulos, T. N.; Neumark, D. M. *J. Chem. Phys.* **1992**, *97*, 6121.
(6) Helden, G.; Gotts, N. G.; Bowers, M. T. *Nature* **1993**, *363*, 60; Gotts, N. G.; Helden, G.; Bowers, M. T. *Int. J. Mass Spectrom. Ion Processes* **1995**, *149/150*, 217.
(7) Zhao, Y.; deBeer, E.; Xu, C.; Taylor, T.; Neumark, D. M. *J. Chem. Phys.* **1996**, *105*, 4905. Zhao, Y.; deBeer, E.; Neumark, D. M. *J. Chem. Phys.* **1996**, *105*, 2575.
(8) Kodama, T,; Kato, T.; Moriwaki, T.; Shiromaru, H., Achiba, Y. *J. Phys. Chem.* **1994**, *98*, 8, 10671. Ohara, M.; Shiromaru, H.; Achiba, Y.; Aoki, K.; Hashimoto, K.; Ikuta, S. *J. Chem Phys.* **1995**, *103*, 10393. Moriwaki, T.; Shiromaru, H.; Achiba, Y. *Z. Phys. D* **1996**, *37*, 169. Ohara, M.; Shiromaru, H.; Achiba, Y. *J. Chem. Phys.* **1997**, *106*, 9992.
(9) Lineberger, W.; Patterson, T. A. *Chem. Phys. Lett.* **1972**, *13*, 40.
(10) Pozniak, B.; Dunbar, R. C. *Int. J. Mass Spectrom. Ion Processes* **1994**, *133*, 97.
(11) Jiao, C. Q.; Phelps, D. K.; Lee, S.; Huang, Y.; Frieser, B. S. *Rapid Commun. Mass Spectrom.* **1993**, *7*, 404.
(12) Forney, D.; Freivogel, P.; Jacobi, M.; Lessen, D.; Maier, J. P. *J. Chem. Phys.* **1995**, *103*, 43. Freivogel, P.; Fulara, J.; Jacobi, M.; Forney, D.; Maier, J. P. *J. Chem. Phys.* **1995**, *103*, 54. Freivogel, P.; Grutter, M.; Forney, D.; Maier, J. P. *J. Chem. Phys.* **1997**, *107*, 22.
(13) Schafer, M.; Grutter, M.; Fulara, J.; Forney, D.; Freivogel, P.; Maier, J. P. *Chem. Phys. Lett.* **1996**, *260*, 406.
(14) Szczepanski, J.; Ekern, S.; Vala, M. *J. Phys. Chem.* **1997**, *101*, 1841.
(15) Freivogel, P; Grutter, M.; Forney, D.; Maier, J. P. *Chem. Phys.* **1997**, *216*, 401.
(16) Raghavachari, K. *Z. Phys. D.* **1989**, *12*, 61; *Chem. Phys. Lett.* **1990**, *171*, 249.

(17) Watts, J. D.; Bartlett, R. J. *J. Chem. Phys.* **1992**, *97*, 3445.
(18) Adamowicz, L. *Chem. Phys. Lett.* **1995**, *182*, 45.
(19) Schmatz, S.; Botschwina, P. *Chem. Phys. Lett*. **1995**, *235*, 5; **1995**, *245*, 136; *Int. J. Mass Spectrom. Ion Processes* **1995**, *149/150*, 621.
(20) Ray, A. K.; Rao, B. K. *Z. Phys. D* **1995**, *197*, 201.
(21) Szczepanski, J.; Wehlburg, C.; Vala, M. *J. Phys. Chem*. **1997**, *101*, 7039; *52nd International Symposium on Molecular Spectroscopy*, Columbus, OH, June 16−20, 1997
(22) Weltner, W., Jr. *Science* **1967**, *155*, 155.
(23) Vala, M.; Chandrashekar, T. M.; Szczepanski, J.; Van Zee, R.; Weltner, W., Jr. *J. Chem. Phys*. **1989**, *90*, 595.
(24) Vala, M.; Chandrashekar, T. M.; Szczepanski, J.; Pellow, R.; *High-Temp. Sci.* **1990,** *27*, 19.
(25) Szczepanski, J.; Vala, M. *J. Chem. Phys.* **1993,** *99*, 7371.
(26) Shen, L. N.; Graham, W. R. M. *J. Chem. Phys*. **1989**, *91*, 5115.
(27) Kranze, R.H.; Graham, W. R. M. *J. Chem. Phys*. **1992**, *96*, 2517; **1993**, *98*, 71.
(28) Kranze, R. H.; Rittby, C. M. L.; Graham, W. R. M. *J. Chem. Phys.* **1995**, *103*, 6841; **1996**, *105*, 5313.
(29) Frisch, M. J.; Trucks, G. W.; Schlegel, H. B.; Gill, P. M. W.; Johnson, B. G.; Robb, M. A.; Cheeseman, J. R.; Keith, T.; Petersson, G. A.; Montgomery, J. A.; Raghavachari, K.; Al-Laham, M. A.; Zakrzewski, V. G.; Ortiz, J. V.; Foresman, J. B.; Cioslowski, J.; Stefanov, B.; Nanayakkara, A.; Challacombe, M.; Peng, C. Y.; Ayala, P. Y.; Chen, W.; Wong, M. W.; Andres, J. L.; Replogle, E. S.; Gomperts, R.; Martin, R. L.; Fox, D. J.; Binkley, J. S.; Defrees, D. J.; Baker, J.; Stewart, J. P.; Head-Gordon, M.; Gonzalez, C.; Pople, J. A. *GAUSSIAN 94*, Revision B.2; Gaussian, Inc.: Pittsburgh, PA, 1995.
(30) Szczepanski, J.; Ekern, S.; Chapo, C.; Vala, M. *Chem. Phys.* **1996,** *210*, 359.